

Electrochemical detection of norepinephrine based on Ag/Fe decorated single walled carbon nanotubes

Xiaojun Hu^{a,b}, Liang Chen^c, Hai Huang^d, Kwangnak Koh^e, Xinluo Zhao^{f,*} & Hongxia Chen^{b,*}

^aState Key Laboratory of Dairy Biotechnology, Bright Dairy & Food Co. Ltd, Shanghai 200444, PR China

^bCenter for Molecular Recognition and Biosensing, School of Life Sciences, Shanghai University, Shanghai 200444, PR China

^cShanghai Biological Science and Technology Co. Ltd, China Stem Cell Group, Shanghai 201821, PR China

^dSchool of Life Sciences, Shanghai University, Shanghai 200444, PR China

^eDepartment of Applied Nanoscience, Pusan National University, Miryang 627-706, Republic of Korea

^fDepartment of Physics, Shanghai University, Shanghai 200444, PR China

Email: xlzhao@shu.edu.cn (XZ)/ hxchen@shu.edu.cn (HC)

Received 12 October 2018; revised and accepted 4 April 2019

A sensitive norepinephrine (NE) sensor using silver and iron nanoparticles decorated single walled carbon nanotubes modified glassy carbon electrode (Ag-Fe/SWCNTs/GCE) for electrochemical detection of trace NE, has been developed. The Ag-Fe/SWCNTs have been prepared using DC arc discharge evaporation and characterized by transmission electron microscope (TEM), scanning electron microscope (SEM) and X-ray diffraction (XRD). The oxidation peak current of NE at Ag-Fe/SWCNTs modified GCE has been greatly increased than that of SWCNTs modified GCE and unmodified GCE. The designed sensor successfully detected NE with good reproducibility and stability, indicating its promising practical applicability. Impressively, the detection limit of NE on Ag-Fe/SWCNTs/GCE has been found to be 5 μM . Owing to the Ag-Fe/SWCNTs specific catalysis of the NE oxidation, NE can be detected selectively in the presence of high concentrations of ascorbic acid (AA). Consequently, this strategy offers a potential, convenient, low-cost, and sensitive sensor for NE diagnosis.

Keywords: Norepinephrine, Electrochemical sensors, Single-walled carbon nanotubes, Silver, Iron, Nanoparticles

Norepinephrine (NE), also called noradrenaline (BAN), is a catecholamine with important physiological effects including those as a neurotransmitter and a hormone¹⁻⁵. NE has an effect on muscle and tissue control, decreases peripheral circulation, stimulates arteriole contraction and activates lipolysis in adipose tissue⁶. There are many diseases related to the changes of its concentration, like Alzheimer and Parkinson. Therefore, it is critical to develop accurate, sensitive and fast methods for the direct determination of NE. So far, various detection methods, such as electrochemical assay⁷⁻¹⁰, spectrophotometry^{11,12}, fluorescence spectroscopy¹³, ion chromatography¹⁴, gas chromatography¹⁵, and high performance liquid chromatography¹⁶, have been employed to analyze NE. Since NE is an electroactive species, electrochemical assay, a simple, practical and reliable method with wide dynamic range and low detection limit, is preferred in comparison to other methods.

In nature, NE coexists with some small biomolecules, such as ascorbic acid (AA)¹⁷. Due to the

overlaid oxidation peak potentials of NE and AA, the separate detection of NE is a challenging work in the presence of AA on conventional unmodified electrodes. Hence, it is necessary to find an efficient method to determine NE with the elimination of the interference of AA. To overcome this problem, it has been proven that the chemically modified electrodes are useful for separate detection of NE and AA. Recently, many materials, including carbon nano-materials¹⁸, amino acids^{19,20}, and metal nanomaterials^{21,22}, have been used to fabricate NE sensors. Taei *et al.*, fabricated a poly-Trypan Blue modified glassy carbon electrode for the simultaneous determination of NE and AA^{23,24}. Mukdasai and coworkers reported a sensitive electrochemical sensor for NE analysis by using gold nanoparticles/multi-walled carbon nanotubes modified glassy carbon electrode consisting of l-cysteine self-assembled monolayers²⁴.

Electrochemical sensing based on carbon nanotubes (CNTs) is a rapidly developing research

field with great scientific appeal. CNTs, with the excellent electrochemical features, can be used in Faradaic processes in view of the fast electron transfer of CNTs, or in non-Faradaic processes like the great changes in conductance^{25,26}. More research and applications on multiwall carbon nanotubes (MWCNTs) exist, than for single-wall carbon nanotubes (SWCNTs), while SWCNTs are well-defined materials in terms of electronic properties compared with MWCNTs. Silver nanomaterials, have led to increased interests and have been intensively used in electrochemistry owing to the excellent electrical conductivity, chemical stability, and electrocatalytic activity²⁷. Chemical decorating is a significant strategy for adjusting the electrical properties of materials^{28,29}. To the best of our knowledge, there are very few reports about using the silver and iron nanoparticles decorated SWCNTs to detect NE and eliminate the interference of AA by electrochemical method.

In this paper, the silver and iron nanoparticles decorated SWCNTs modified glassy carbon electrode (GCE) was prepared to fabricate a novel sensor for the determination of NE. The results exhibited the superiority of the modified GCEs in comparison to the bare electrodes with respect to the improvement of reversibility and sensitivity. Moreover, this modified electrode also showed the well-separated oxidation peaks of NE and AA in buffer solution, which was demonstrated to be an effective strategy with simplicity, selectivity, stability and fast response.

Materials and Methods

All chemicals used were of analytical reagent grade and were used as received. PE was purchased from Korea (Darmstadt, Germany). Ascorbic acid was purchased from Sigma–Aldrich (USA). Doubly-distilled water was used throughout the whole study. All cyclic voltammetric experiments were performed at the ambient temperature (25 °C). Electrochemical measurements were carried out by an electrochemical analyser (CHI 660 D, CHI Shanghai, Inc.) connected to a personal computer. The metal nanoparticles and the morphology of the nanotubes were studied by transmission electron microscope (TEM, JEOL JEM-200CX) and scanning electron microscope (SEM, FESEM, JEOL JSM-6700F). X-ray diffraction (XRD) instrument (Rigaku Corporation DLMAX-2200) was employed to characterize the structures of the samples in the range of 25°–85° at a scanning speed of 1° min⁻¹. A three-electrode configuration was used, which consists of a bare or modified GCE (3 mm in

diameter) as a working electrode and an Ag/AgCl saturated KCl electrode and a platinum wire (1 mm in diameter) as the reference electrode and auxiliary electrode, respectively.

Phosphate buffer solutions (PBS, 0.1 M) were prepared with different pH values (5.5, 6.0, 6.5, 7.0, 7.5, and 8.0). A 2.0 mM NE solution was prepared by dissolving 159.63 mg NE in PBS with different pH values. A series of dilute solutions were obtained by serial dilution with PBS. A 2.0 mM AA solution was prepared by using the same method to the preparation of NE solution.

Preparation of Ag-Fe/SWCNTs

The Ag-Fe/SWCNTs were prepared by a method similar to that of DC arc discharge evaporation³⁰. The cathode and anode were horizontally installed at the center of a water-cooled chamber. The anode was a carbon rod doped with Ag (0.5 at.%) and Fe (1 at.%) catalyst (10 mm in diameter, 70 mm in length), and the cathode was a pure carbon rod (10 mm in diameter, 30 mm in length). We applied 90 A to generate the DC arc discharge in H₂-Ar atmosphere. The distance between two electrodes was kept constant at approximately 2 mm. SWCNTs were generated with Fe catalyst and Ag nanoparticles were loaded on the surface of SWCNTs by arc discharge evaporation. Ag loading and SWCNTs growth occurred almost simultaneously. Before electrochemical measurement, Ag-Fe/SWCNTs were heated at 800 °C for 2 h to remove the amorphous carbon in H₂-Ar mixture gas.

Preparation of Ag-Fe/SWCNTs film modified electrode

By ultrasonic agitation, 0.5 mg of purified Ag-Fe/SWCNTs was dispersed in 1 mL of mixed solution, which contains 0.5 mL acetone and 0.5 mL *N,N*-dimethylformamide (DMF) to give a 0.5 mg/mL suspension liquid. The GCE was abraded carefully with emery paper (No.5000 and No.3000) and chamois leather containing 0.05 mm aluminum slurry, and then washed ultrasonically with distilled water and ethanol respectively. The SWCNTs film was prepared through dropping SWCNTs (0.1 mg/mL) in DMF and acetone using microsyringe on the surface of GCE, and then the solvent was evaporated under an infrared heat lamp for 2 min. The prepared electrode was denoted as Ag-Fe/SWCNTs/GCE.

Electrochemical detection

A 0.1 M PBS of pH 6.5 was selected as the supporting electrolyte to determine NE and AA. The

Ag-Fe/SWCNTs/GCE was activated by 7 consecutive cyclic voltammetric potential sweeps between -0.2 V and 1.6 V at 100 mV/s in the blank PBS (pH 6.5) before the measurement. At room temperature, cyclic voltammogram (CV) was recorded in a potential range of -0.2 – 0.8 V at a scan rate of 100 mV/s at the CHI 660 C electrochemical workstation. The reductive current at 0.32 V was used as the signal for the determination of NE.

Results and Discussion

Characterization of the synthesized nanomaterials

A typical SEM image and EDS analysis of the purified Ag-Fe/SWCNTs is given in Fig. 1a and Table 1. The SWCNT bundles are crossed with each other and form into a network loaded with metal nanoparticles as the bright spots. The EDS results reveal that Ag and Fe coexist in the sample (Table 1). Because of some sulfur existing in the raw carbon powders, sulfur also appeared besides carbon, Ag and Fe. The TEM image of Ag-Fe/SWCNTs before purification is given in Fig. 1b. For the as-grown sample, the metal nanoparticles, the dark spots of the surface of SWCNTs bundles, are dispersed homogeneously, and surrounded or encapsulated by amorphous carbon and carbon shells. According to previous works, the diameters of Ag and Fe

nanoparticles are in the range of 1 to 10 nm^{31,32}. The Raman spectra of the purified Ag-Fe/SWCNTs are given in Fig. 1c. SWCNTs have three characteristic vibrational modes of low-frequency radial breathing mode (RBM, 100 – 300 cm⁻¹), high-frequency tangential mode (G-band, around 1580 cm⁻¹), and the D-band (around 1350 cm⁻¹). The G-band is the only band which arises from a first-order Raman scattering process, related to phonon vibrations in sp^2 carbon materials, and the D band is attributed to the disordered structures. The intensity ratio of the D and G band (I_D/I_G) can be used to describe the crystallinity and the relative amount of amorphous carbon for the SWCNTs samples. The lower the I_D/I_G value, the higher the purity of the sample. The diameters of SWCNTs, namely d_t , was calculated by the following equation:

$$\omega_{\text{RBM}} = 234/d_t + 10 \text{ cm}^{-1} \quad \dots(1)$$

where ω_{RBM} (cm⁻¹) is the wave number of the radial breathing mode (RBM) in the Raman spectrum³³.

Table 1 — EDS analysis of the purified Ag-Fe/SWCNTs

Element	C	O	S	Fe	Ag
Atom ratio (at%)	37.23	7.40	4.11	26.19	25.08
Mass ratio (wt%)	9.19	2.43	2.71	30.06	55.61

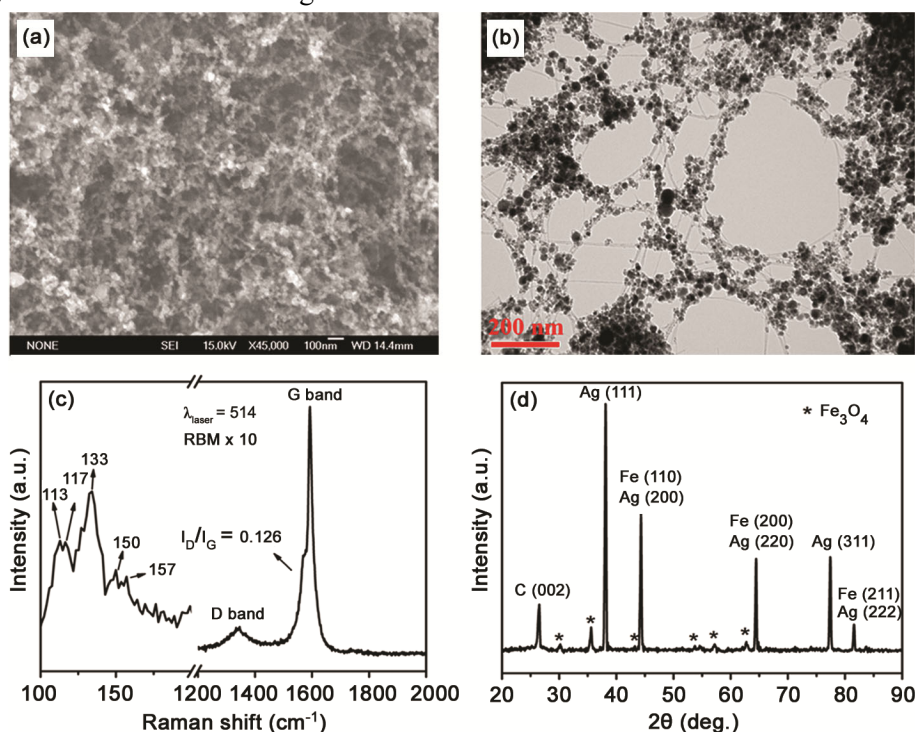


Fig. 1 — (a) SEM image of the purified Ag-Fe/SWCNTs, (b) TEM image of Ag-Fe/SWCNTs before purification, (c) Raman spectra of the purified Ag-Fe/SWCNTs, and, (d) XRD patterns of Ag-Fe/SWCNTs.

Several RBM peaks appears in the range of 110 to 157 cm^{-1} , corresponding to a diameter range of 1.6 to 2.3 nm. For the XRD patterns of the purified Ag-Fe/SWCNTs, the diffraction peaks at 2θ (diffraction angle) = 38.12°, 44.33°, 64.46°, 77.39°, and 81.56° can be assigned to Ag (111), Ag (200), Ag (220), Ag (311), and Ag (222), respectively (Fig. 1d). The Fe (110), Fe (200), and Fe (211) showed that the corresponding diffraction peaks at 44.35°, 64.53°, and 81.65°, almost overlapped with the peaks of Ag (200), Ag (220), and Ag (222). Some peaks of Fe_3O_4 appeared because carbon impurities that encapsulated the metal nanoparticles were removed by H_2 treatment, and Fe nanoparticles were oxidized by oxygen when the Ag-Fe/SWCNTs were taken out and exposed to air. From the XRD results, the Ag nanoparticles were not oxidized.

Electrochemical characterization of NE at the Ag-Fe/SWCNTs modified GCE

In order to compare the detection effect of Ag-Fe/SWCNTs modified GCE on NE, the modified GCE and the bare GCE were placed in 2.0 mM NE solution (pH 6.5). As a result, NE showed a higher redox peak current on the modified GCE of Ag-Fe/SWCNTs (Fig. 2), and $\Delta E_p = \text{oxidation peak} - \text{reduction peak} = \Delta E_{pa} - \Delta E_{pc} = 0.326 \text{ V} - 0.189 \text{ V} = 137 \text{ mV}$. The decrease in the potential difference indicates that the electron transfer rate was accelerated. The oxidation-reduction reaction is equal to that of the bare GCE and $\Delta E_{pa} - \Delta E_{pc} = 249 \text{ mV} = \text{the enhancement of the reversibility of silver}$, that is, the modified GCE of Ag-Fe/SWCNTs has a good effect on NE. The reason is that the carbon nanotubes have a very high aspect ratio and catalytically active surface, and single-walled carbon nanotubes increase

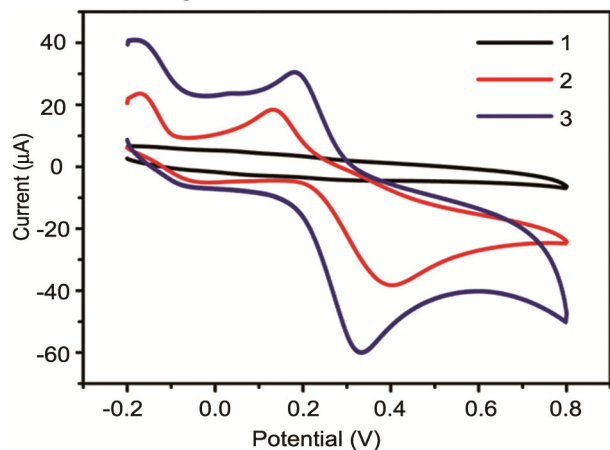


Fig. 2 — CVs at a bare GCE in 0.1 M PBS of pH 6.5 (curve 1), and bare GCE in 2 mM NE (curve 2) and Ag-Fe/SWCNTs/GCE in 2 mM NE (curve 3) [scan rate: 100 mV/s].

the surface area of the electrode, which lead to the greatly increased background current than for the bare electrode. On the other hand, silver nanomaterials have small particle size with specific surface area, different electronic state of the surface and the interior, excellent conductivity, and strong catalytic effect. The above results prove that Ag-Fe/SWCNTs can be used as a substrate for sensitive detection of NE.

Optimization of detection conditions

NE is known to be deprotonated or protonated with solutions having different pH. To demonstrate the influence of pH on the peak current of NE, the curve of the peak current versus pH was plotted by cyclic voltammetry in PBS at pH 5.5 to 8.0. It can be seen that at about pH 6.5, the anodic peak current has the highest value, indicating the best response of NE under this condition (Supplementary Data, Fig. S1a). Therefore, pH 6.5 was used in our experiments. In addition, the CVs of NE for different amounts of Ag-Fe/SWCNTs modified GCE were investigated to explore the optimized condition of electrode modification. As shown in Fig. S1b, the maximum oxidation peak current of NE at Ag-Fe/SWCNTs modified GCE was 63.6 μA , which is larger than that at SWCNTs modified GCE. This indicates that the silver nanoparticles attached on the SWCNTs could facilitate electron transfer of NE.

The effect of the scan rate on electrochemical behaviours of NE was investigated by recording the CVs of 2 mM NE on Ag-Fe/SWCNTs/GCE at different scan rates from 20 to 200 mV/s in PBS of pH 6.5 (Fig. 3a). It can be seen that anodic peak current was linear with the scan rate (Fig. 3b). The linear regression equation is $I_{pa} (\mu\text{A}) = -2.95 \times 10^{-6} + 6.66 \times 10^{-8} \text{ V (mV/s)}$ with $r^2 = 0.996$, suggesting that the redox reaction of NE involved an adsorption-controlled process according to Laviron *et al.*³⁴. The peak current increased with the scan rate, and simultaneously the peak-to-peak separation (ΔE_p) also increased, which revealed a quasi-reversible electron transfer process. Taking into account the sensitivity of Ag-Fe/SWCNTs modified GCE, the scan rate of 100 mV/s was selected for the whole experiment. Owing to the NE adsorption on the surface of Ag-Fe/SWCNTs/GCE, the adsorption time had an enormous influence on the peak current. Hence, the influence of adsorption time was studied, which manifested that the peak currents reached the maximum level when the Ag-Fe/SWCNTs/GCE was put into 2 mM NE for more than 5 min.

NE detection

Sensitivity is a significant criterion to assess NE detection method. The CVs recorded at different concentrations of NE in the range of 0.005 mM to 2 mM in pH 6.5 PBS buffer is given in Fig. 4a. The peak current increases with increasing NE concentration. The linear relationship was found as shown in Fig. 4b, i.e., $I_{pa} = 33.8C(NE) + 11.1$, $r^2 = 0.964$ in the range of 50 μM to 500 μM . When the concentration of NE was 5 μM , Ag-Fe/SWCNTs modified GCE could promote its electrochemical behavior, that is, the detection limit of NE was 5 μM .

Sensor's selectivity

As mentioned above, the Ag-Fe/SWCNTs/GCE has high electrocatalytic activity toward the oxidation of NE, which can be used as a chemically modified electrode to explore analytical and biological applications. In this study, detection of biomolecule AA was also analysed on this electrode besides NE. The irreversible oxidation peak was at 0.2 V on the bare GCE, but peak potential shifted to 0.33 V with reduced

peak current on the Ag-Fe/SWCNTs/GCE (Fig. 5a). Hence, it is clear that the Ag-Fe/SWCNTs/GCE cannot catalyze the oxidation of AA. When 1 mM NE was added to the above system, there was only one oxidation peak on the bare electrode (Fig. 5b), indicating that the bare GCE was not effective in detecting NE in the presence of AA. Whereas, two oxidation peak potentials were observed on Ag-Fe/SWCNTs modified GCE. The first one was the oxidation peak potential of AA and the second one was close to NE oxidation peak potential. Based on this, NE assays can be performed selectively in the presence of high concentrations of AA ($C_{AA} = C_{NE}$).

For the study of stability of the Ag-Fe/SWCNTs film modified GCE, the experimental results showed the CV curves of 2 mM NE (pH 6.5) are similar to those of Ag-Fe/SWCNTs modified by the same GCE, and the relative standard deviation (RSD) of the oxidation peak current is 0.2% (Table S1). The CV curves of 2 mM NE (pH 6.5) exhibited that the RSD

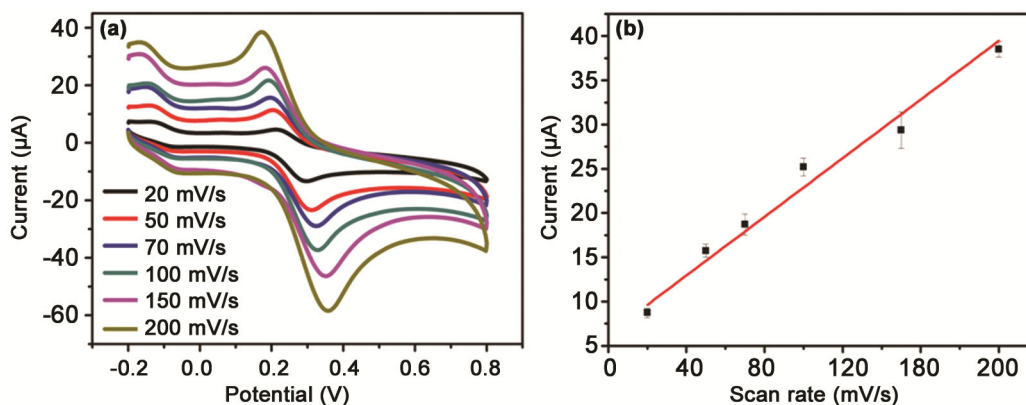


Fig. 3 — (a) CVs of 2 mM NE on the Ag-Fe/SWCNTs modified GCE in 0.1 M PBS of pH 6.5 at different scan rates (20, 50, 70, 100, 150 and 200 mV/s), and, (b) relationship of the redox peak currents of NE and the scan rate.

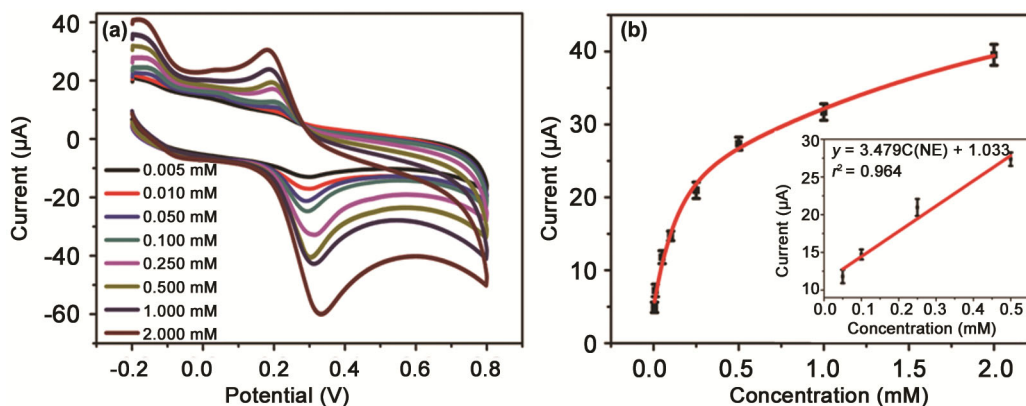


Fig. 4 — (a) CVs of different concentrations (from 0.005 mM to 2 mM) of NE in PBS of pH 6.5 on the Ag-Fe/SWCNTs modified GCE, and, (b) relationship of redox peak currents and concentrations of NE.

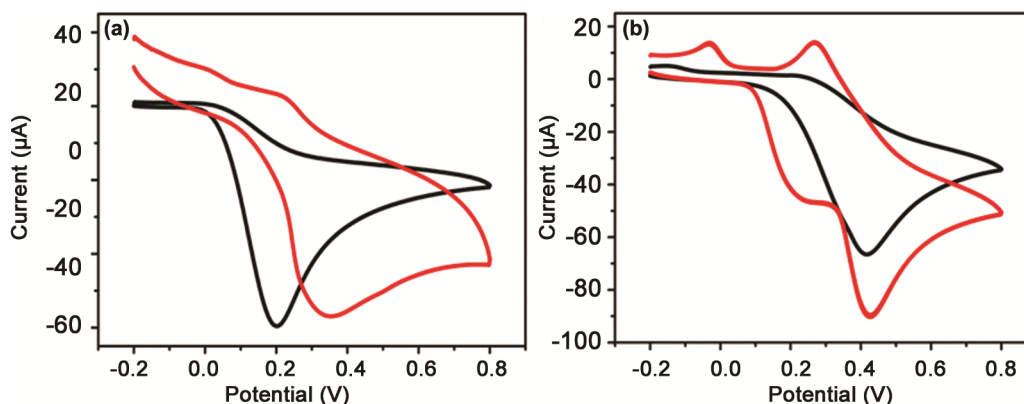


Fig. 5 — CVs of 2 mM AA on the bare GCE (black) and Ag-Fe/SWCNTs/GCE (red) (a) without and (b) with 1 mM NE in 0.1 M PBS of pH 6.5 [scan rate: 100 mV/s].

of the oxidation peak current was 1.2% when the Ag-Fe/SWCNTs modified three different GCEs in parallel experiments (Table S2). The results manifested that the reproducibility of Ag-Fe/SWCNTs modified GCE is very satisfying. Additionally, long-term stability experiments were studied by storing the proposed electrodes at 4 °C and measuring their electrochemical signal every five days (Supplementary Data, Fig. S2). Even after storing for 30 days, the electrochemical signal essentially maintains its original current response. These results confirmed that the prepared sensor showed good stability and reproducibility.

From literature, numerous methodologies for NE detection have been exploited. In some cases, the process of sensor fabrication is a tedious one involving in the use of hazardous precursor materials or organic solvents, or the fabrication is expensive and time consuming. The comparison of our developed Ag-Fe/SWCNTs/GCE sensor with other NE detection sensors, shows that the sensor system using SWCNTs is low-cost and easy to synthesize. Moreover, it can be effectively used to separate NE and AA. Consequently, this system is a better candidate for the selective and sensitive detection of NE in aqueous solution.

Conclusions

A sensitive sensor was designed for NE detection on the basis of silver and iron nanoparticles decorated single walled carbon nanotube modified glassy carbon electrode. The fabricated Ag-Fe/SWCNTs/GCE detected NE in the linear range of 50 to 500 μM with an LOD of 5 μM . The proposed sensor successfully analysed the presence of NE with good reproducibility, revealing its promising practical applicability,

and also efficiently exhibited the separation of NE and AA. However, the preparation process of Ag-Fe/SWCNTs needs harsh reaction conditions and needs to be carried out at 800 °C, which may limit the laboratory study and applications of this material.

Supplementary Data

Supplementary data associated with this article are available in the electronic form at [http://www.niscair.res.in/jinfo/ijca/IJCA_58A\(05\)547-553_SupplData.pdf](http://www.niscair.res.in/jinfo/ijca/IJCA_58A(05)547-553_SupplData.pdf).

Acknowledgement

This work was supported by State Key Laboratory of Dairy Biotechnology, Bright Dairy & Food Co. Ltd (SKLDB2016-001), Shanghai Biological Science and Technology Co. Ltd., China Stem Cell Group (D71011217014), and the National Natural Science Foundation of China (Grant No. 61875114).

References

- Xu Z, Zhang Z J, Shi Y Y, Pu M J, Yuan Y G, Zhang X R & Li L J, *J Affect Disord*, 133 (2011) 165.
- Spencer W A, Jeyabalan J, Kichambre S & Gupta R C, *Free Radic Biol Med*, 50 (2011) 139.
- Kania B F & Sutiak V, *Res Vet Sci*, 90 (2011) 291.
- Ribeiro J A, Fernandes P M, Pereira C M & Silva F, *Talanta*, 160 (2016) 653.
- Nada F A & Maher F E, *Talanta*, 79 (2009) 639.
- Raj M A & John S A, *Anal Methods*, 6 (2014) 2181.
- Mazloum-Ardakani M, Beitollahi H, Sheikh-Mohseni M A, Naeimi H & Taghavini N, *Appl Catal A Gen*, 378 (2010) 195.
- Mazloum-Ardakani M, Beitollahi H, Amini M K, Mirkhalaf F & Mirjalili B, *Biosens Bioelectron*, 26 (2011) 2102.
- Dong H, Wang S, Liu A, Galligan J J & Swain G M, *J Electroanal Chem*, 632 (2009) 20.
- Jin G P, Peng X & Ding Y F, *Biosens Bioelectron*, 24 (2008) 1031.
- Chen J, Huang H & Zeng Y, *Biosens Bioelectron*, 65 (2015) 366.

- 12 Zhu M, Huang X M, Li J & Shen H X, *Anal Chim Acta*, 357 (1997) 261.
- 13 Ma Y, Yang C, Li N & Yang X, *Talanta*, 67 (2005) 979.
- 14 Guan C L, Ouyang J, Li Q L, Liu B H & Baeyens W R G, *Talanta*, 50 (2000) 1197.
- 15 Cramer S C, *Stroke*, 46 (2015) 2998.
- 16 Allen S A, Rednour S, Shepard S & Pond B B, *Biomedical Chromatogr*, 31 (2017) e3998.
- 17 Zaidi S A, *Sens Actuators B Chem*, 265 (2018) 488.
- 18 Huang S H, Liao H H & Chen D H, *Biosens Bioelectron*, 25 (2010) 2351.
- 19 Zhan L, Sun Y & Lin X, *Analyst*, 6 (2001) 60.
- 20 Goyal R N, Aziz M A, Oyama M, Chatterjee S & Rana A R S, *Sens Actuators B: Chem*, 53 (2011) 232.
- 21 Yang Z, Hu G, Chen X, Zhao J & Zhao G, *Coll Surf B*, 54 (2007) 230.
- 22 Li C Y, Cai Y J, Yang C H, Wu C H, Wei Y, Wen T C, Wang T L, Shieh Y T, Lin W C & Chen W J, *Electrochim Acta*, 56 (2011) 1955.
- 23 Taei M & Jamshidi M S, *J Microchem*, 130 (2017) 108.
- 24 Mukdasai S, Langsi V, Pravda M, Srijaranai S & Glennon J D, *Sens Actuators B: Chem*, 236 (2016) 126.
- 25 Gupta S, Murthy C N & Ratna Prabha C, *Int J Biol Macromol*, 108 (2018) 687.
- 26 Alam A U, Qin Y, Howlader M, Hu N & Deen M J, *Sens Actuators B: Chem*, 254 (2018) 896.
- 27 Movahedi E & Rezvani A, *Anal Bioanal Electrochem*, 9 (2017) 956.
- 28 Emran M Y, Khalifa H, Goma H, Shenashen M A, Akhtar N, Mekawy M, Faheem A & El-Safty S A, *Microchim Acta*, 184 (2017) 4553.
- 29 Maluta J R, Machado S A S, Chaudhary U, Manzano J S, Kubota L T & Slowing I I, *Sens Actuators B: Chem*, 257 (2018) 347.
- 30 Liu X, Yu L & Liu F, *J Mater Sci*, 47 (2012) 6086.
- 31 Chan S C & Barteau M A, *Langmuir*, 1 (2005) 588.
- 32 Wang L, Ji H M & Wang S, *Nanoscale*, 5 (2013) 93.
- 33 Dresselhaus M S, Dresselhaus G, Saito R & Jorio A, *Phy Rev*, 409 (2005) 47.
- 34 Laviron E, *Chem*, 101 (1979) 19.